Synthesis of alginate beads filled with nanohydroxyapatite: An efficient approach for fluoride sorption

Kalimuthu Pandi, Natrayasamy Viswanathan

Department of Chemistry, Anna University, University College of Engineering-Dindigul, Dindigul-624 622, Tamil Nadu, India
Correspondence to: N. Viswanathan (E-mail: drnviswanathan@gmail.com)

ABSTRACT: Nanohydroxyapatite (n-HAp) powder is a promising adsorbent material with high defluoridation capacity (DC); however, it causes pressure drop during field applications. To overcome such problems and utilize the advantages of n-HAp, it is aimed to prepare n-HAp in a usable bead form with the support of alginate (Alg) biopolymer. n-HApAlgLa composite beads were synthesized by introducing n-HAp powder in Alg polymeric gel, and the resulting solution was dropped into La^{3+} ions for crosslinking. Defluoridation experiments were carried out in batch mode to optimize various influencing parameters like contact time, pH, challenger anions, initial fluoride concentrations, and temperature. The beads were characterized using Fourier transform infrared spectroscopy, X-ray diffraction, and scanning electron microscopy with energy-dispersive X-ray analyzer analysis. The sorption process was explained using diverse isotherms and kinetic models. The values of thermodynamic parameters indicate that the nature of fluoride is spontaneous and endothermic in nature. In field studies, n-HApAlgLa beads reduce the fluoride concentration below the tolerance limit. The regeneration and reusability studies were proposed to effectively use the sorbent. © 2015 Wiley Periodicals, Inc. J. Appl. Polym. Sci. **2015**, *132*, 41937.

INTRODUCTION

Fluoride enters into water mainly through fluoride-bearing minerals and from industrial effluents. Drinking water is the key source of fluoride intake. The excess fluoride content (>1.5 mg L^{-1}) in drinking water leads to fluorosis.[1] Hence, it is an important task to supply water with safe fluoride levels. Defluoridation is one of the best options to reduce fluoride concentration in water. Researchers actively involved in removing the excess fluoride from water, which includes precipitation, reverse osmosis, electrocoagulation, nanofiltration, ion exchange, and adsorption.[2–8] Among the methods reported, adsorption has been identified as the effective approach for fluoride removal.

Hydroxyapatite (HAp) is a biocompatible material and potential adsorbent for the removal of toxic ions and organic pollutants in water.[9] Nowadays, the research studies have been focused on nanohydroxyapatite (n-HAp) because of its high surface area and reactivity.[10] However, the application of n-HAp in adsorption columns is limited because of its powder form, insufficient strength, and brittleness. To triumph over such technological troubles, polymeric composites have been developed. The inorganic materials like HAp, alumina, and clays modified using polymers will generate polymeric composites, which possess the unique properties such as rigidity, hardness, and mold shrinkage for the development of technology.

Currently, biosorption plays a vital role in minimizing the environmental pollution.[11–13] Alginate (Alg) is a biopolymer isolated from brown seaweeds, which is biocompatible, biodegradable, nontoxic, and an inexpensive material. Recently, Alg-supported nanocomposites and functionalized Alg materials were used for the removal of toxic ions from the aqueous solution.[14–19] However, Ca^{2+} ions crosslinked with Alg beads are unstable because of the replacement of Ca^{2+} ions with H^+ ions in acidic environment which decrease their performance.[20] To enhance the stability, adsorption capacity, and reusability, high-valence metal ions are used as crosslinking agents to design the biocomposite beads.[21] Recently, the adsorbents with rare earth elements are being paid more interest because of their selectivity, high adsorption capacity, minimum pollution, and easy operation.[22,23]

Hence, this research investigation aimed to synthesize of composite beads by incorporating n-HAp in the Alg polymatrix followed by crosslinking with La^{3+} ions. The developed n-HApAlgLa composite beads were used for fluoride removal in batch mode. Various sorption-influencing parameters like contact time, pH, presence of competitor anions, different initial fluoride concentrations, and temperature have been optimized for maximum fluoride removal. Sorption data have been fitted to various isotherms and kinetic models. The thermodynamic parameters, namely, $\Delta G°$, $\Delta H°$, and $\Delta S°$ have been calculated to
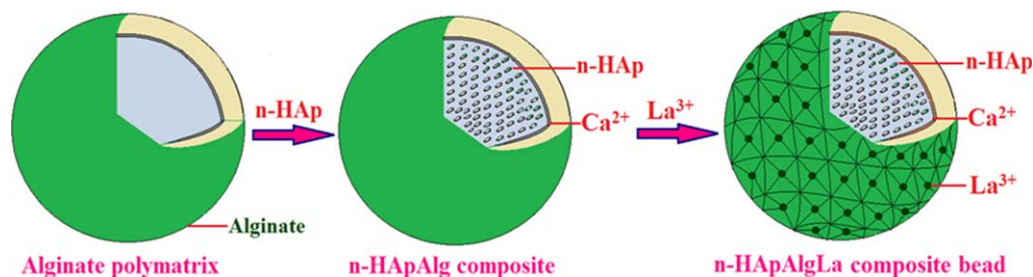
Figure 1. Synthesis of n-HApAlgLa composite beads. [Color figure can be viewed in the online issue, which is available at wileyonlinelibrary.com.]

find the nature of fluoride sorption. The suitability of the composite beads at field conditions was also tested by collecting field fluoride water sample from nearby fluoride widespread area.

MATERIALS AND METHODS

Materials

Sodium alginate with a molecular weight of 70,000–80,000 was purchased from Himedia (India). Calcium nitrate tetrahydrate, ammonium dihydrogen phosphate, lanthanum chloride heptahydrate, 25% ammonia solution, and potassium bromide were purchased from Merck (Mumbai, India). Sodium fluoride (ACS grade, >99%) was purchased from Merck (Mumbai, India), and all the reagents were used without further purification. Double distilled water was used to prepare the standard solutions.

Preparation of n-HApAlgLa Composite Beads

n-HAp powder was prepared by chemical coprecipitation method according to the method proposed by Sairam Sundaram et al.[24] About 2 g of n-HAp powder was uniformly dispersed in 100 mL of distilled water. During dispersion, the n-HAp particles tended to agglomerate in water, and the dispersing process was well assisted by sonication for 30 min and followed by mechanical stirring for 1 h. After obtaining the complete dispersion solution, 2 g of sodium alginate was added into n-HAp solution and stirred vigorously for 3 h. The resulting homogeneous n-HApAlg solution was dropped into 0.2 mol L^{-1} of $LaCl_3 \cdot 7H_2O$ solution to get n-HApAlgLa beads. For complete crosslinking reaction, the beads were left for 24 h in La^{3+} solution. Later, the composite beads were thoroughly washed with distilled water and then dried at 80°C in hot-air oven for 10 h and were used for sorption studies. The feasible reaction scheme is shown in Figure 1.

Fluoride Removal Experiments

Defluoridation studies were carried out in the batch equilibration method in duplicate. The experiments were conducted by adding 0.1 g of dry beads into 50 mL of 10 mg L^{-1} sodium fluoride solution at room temperature with neutral pH. The influence of pH on the sorption of fluoride by n-HApAlgLa beads were studied by varying the pH of the solution in the range of 3–11 using 0.1M HCl/NaOH solution. The mixture was shaken in an orbital shaker with a speed of 200 rpm at room temperature. The samples were taken at prefixed time intervals for the analysis of fluoride concentrations in the solutions until sorption equilibrium was reached. Thermodynamic studies were car-

ried out using a waterbath shaker with different initial fluoride concentrations, namely, 8, 10, 12, and 14 mg L^{-1} in the temperature range of 30, 40, and 50°C at neutral pH. After equilibration, the samples were filtered, and the final fluoride concentration was determined. The defluoridation capacity (DC) of the material was calculated by the following equation:

$$\text{Defluoridation capacity (DC)} = \frac{C_i - C_e}{m} V \times 1000 \ \text{mgF}^- \text{kg} \quad (1)$$
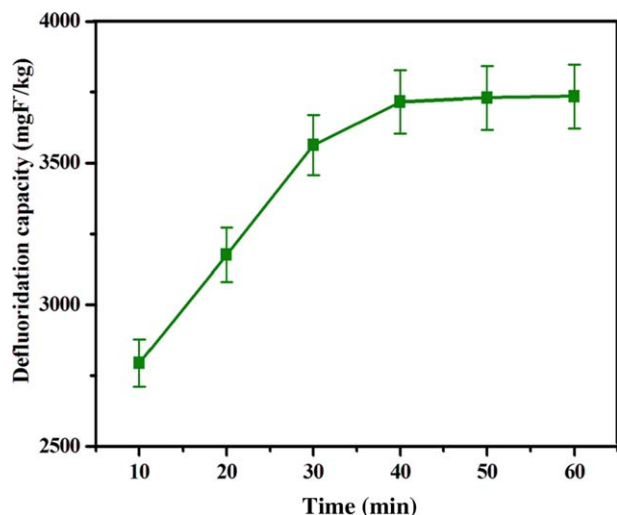
where C_i is the initial fluoride concentration (mg L^{-1}), C_e is the equilibrium fluoride concentration (mg L^{-1}), m is the mass of the adsorbent (g), and V is the volume of the solution (L).

Analysis

The fluoride concentration was measured using Thermo Orion Benchtop multiparameter kit (Model: VERSA STAR 92) with the fluoride ion selective electrode (9609 BNWP), with the relative accuracy of ±1 significant digit, detection limit of 0.02 mg L^{-1}, and the reproducibility of ±2% (Thermo Orion, USA). The pH measurements were made with the same instrument using pH electrode. All other water quality parameters were analyzed using standard methods.[25] The pH at zero point charge (pH_{zpc}) of the composite beads was determined by pH drift method.[26]

Instrumental Analysis

Fourier transform infrared (FTIR) spectra of the composite beads were carried out by JASCO-460 plus spectrometer operated at 1 cm^{-1} resolution in the range of 400–4000 cm^{-1}. n-HApAlgLa composite beads (before and after fluoride sorbed) was ground in agate mortar and mixed with KBr at a ratio of 1/400. The pellets were generated by pressing at 10 tons cm^{-2} for 3 min with a hydraulic press under vacuum. Scanning electron microscopy (SEM) with energy-dispersive X-ray analyzer (EDAX) is one of the best known and most widely used surface analytical techniques. The surface morphology of the beads was imagined by SEM with Vega3 Tescan model operating at 30.0 kV. The SEM facilitates the direct observation of the surface microstructures of the fresh and fluoride-sorbed beads. Elemental spectra of the composite beads were obtained using an EDAX (Bruker Nano GMBH, Germany) during SEM observations, which allow a qualitative detection and localization of elements in the composite beads. X-ray diffraction (XRD) measurements were obtained using X'per PRO model-PANalytical to determine the crystalline phases present in the sorbent at a scan rate of 0.5 min^{-1} with Cu Kα radiation (1.54

Figure 2. Effect of contact time on the DC of n-HApAlgLa composite beads in the presence of 10 mg L^{-1} initial fluoride concentration and 0.1 dosage with neutral pH at room temperature. [Color figure can be viewed in the online issue, which is available at wileyonlinelibrary.com.]

Figure 3. Influence of initial pH on the DC of n-HApAlgLa composite beads in the presence of 10 mg L^{-1} initial fluoride concentration and 0.1 dosage with 40 min contact time at room temperature. [Color figure can be viewed in the online issue, which is available at wileyonlinelibrary. com.]

Å) and a secondary beam graphite monochromator. The data were recorded over the angular range from 0 to 70° (2θ).

Statistical Tools

The computations were done using Microcal Origin (Version 8.0) software. The goodness of the fit and best model was discussed using error bar plot, regression correlation coefficient (r), chi-square analysis (χ^2), and standard deviation (SD).
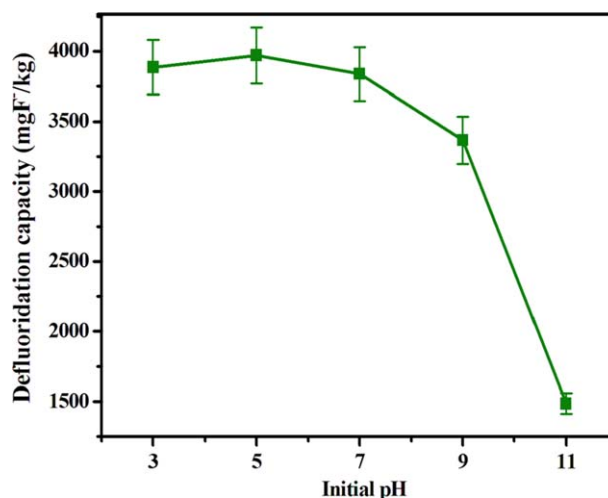
RESULTS AND DISCUSSION

Effect of Contact Time on the Sorption of Fluoride

To find out the minimum contact time for the maximum DC, sorption experiments were carried out by the varying contact time in the range of 10–60 min with 10 mg L^{-1} initial fluoride concentration and 0.1 g as dosage at neutral pH. Figure 2 shows that the sorption of fluoride by n-HApAlgLa beads were hasty and reached saturation at 40 min. The result shows that n-HApAlgLa beads possessed an enhanced DC of 3716 mgF^{-} kg^{-1}. Therefore, 40 min of equilibrium contact time was chosen as the period of contact time for the successive experiments.

Performance of Composite Beads at Different pH Medium

The solution pH is one of the important factors that influence the uptake capacity of fluoride in the water-adsorbent interface. The removal of fluoride by n-HApAlgLa beads were studied with different initial pH ranges from 3 to 11, by keeping all other parameters as constant. As evident from Figure 3, the sorption of fluoride onto the beads was increased from pH 3 to 5, because at lower solution pH, more protons combine with fluoride leading to the formation of hydrogen fluoride, which leads to unfavorable adsorption of fluoride onto beads. When moving toward higher pH ranges (pH 5–11), the DC decreases with increase in solution pH. The main reason could be that at higher pH ranges, the hydroxyl ions may also compete with fluoride ions in the active sites of the beads during sorption.[27] Irrespective of the initial pH solution, after treatment with n-HApAlgLa beads, the pH of the solution becomes neutral, indi-

cating that n-HApAlgLa composite beads can be used in all types of pH environment (i.e., acidic, basic, and neutral), which is one of the advantages of this composite material.

Effect of Challenger Anions During Fluoride Sorption

Normally, the drinking water contains other anions like Cl$^-$, NO$_3^-$, SO$_4^{2-}$, and HCO$_3^-$ ions. To know the effect of these challenger anions on fluoride sorption, it was investigated with 200 mg L^{-1} as initial concentrations of these ions, 10 mg L^{-1} as the initial fluoride concentration, and by keeping all other parameters as constant. Figure 4 shows that there is no significant change in fluoride uptake capacity in the presence of the challenger anions like Cl$^-$, NO$_3^-$, and SO$_4^{2-}$ ions. However,
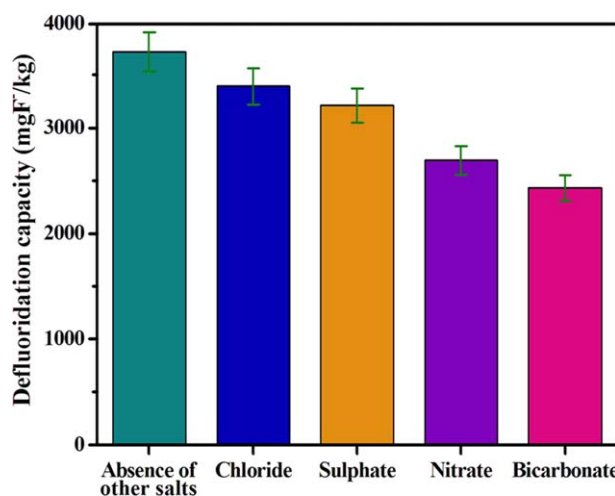
Figure 4. Effect of challenger anions on the DC of n-HApAlgLa composite beads in the presence of 10 mg L^{-1} initial fluoride concentration, 200 mg L^{-1} other anion concentration, and 0.1 dosage with neutral pH at room temperature. [Color figure can be viewed in the online issue, which is available at wileyonlinelibrary.com.]
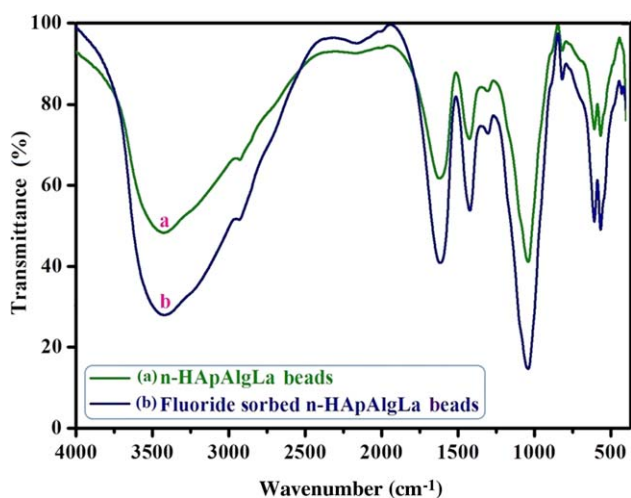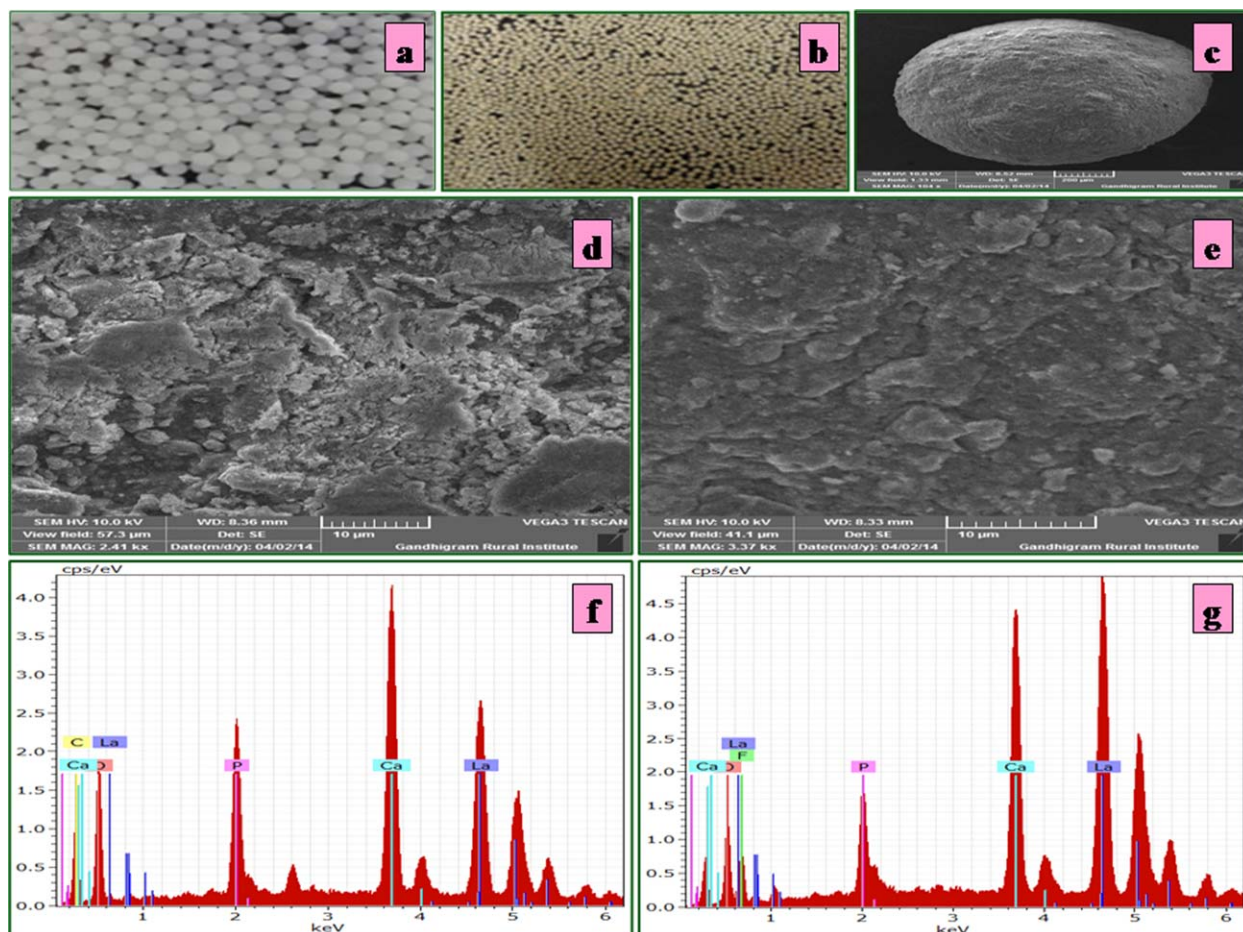
Figure 5. FTIR spectra of (a) n-HApAlgLa beads and (b) fluoride-sorbed n-HApAlgLa beads. [Color figure can be viewed in the online issue, which is available at wileyonlinelibrary.com.]

the DC of the composite beads decreases in the presence of HCO_3^- ion, because the increase in solution pH simultaneously reduces the active sites for fluoride sorption.[28]

Characterization of the Composite Beads

Figure 5 illustrates the FTIR spectra of synthesized n-HApAlgLa beads and fluoride-treated n-HApAlgLa beads. The strong absorption band observed at 552 and 1035 cm^{-1} indicates the bending and stretching vibration of PO_4^{3-} in n-HAp.[29] In addition, Alg also has a strong band at 1035 cm^{-1}.[30] The observed broadband at 1035 cm^{-1} is attributed to the overlap of C—O—C stretching of Alg and PO_4^{3-} stretching of n-HAp. In n-HApAlgLa composite, the observed bands at 1616 and 1423 cm^{-1} suggests the formation of the chemical bond between the mineral phase and the organic matrix, that is, the interaction between La^{3+} ion and the carboxyl group of Alg.[31] The band at 3446 cm^{-1} is assigned to stretching vibration of the —OH groups of Alg and n-HAp. The broadening of the band at 3446 cm^{-1} in the fluoride-sorbed n-HApAlgLa beads are due to electrostatic adsorption between the sorbent and the fluoride ion.

The digital images of wet and dry n-HApAlgLa composite beads are shown in Figure 6(a,b), respectively. The SEM image of single n-HApAlgLa bead is shown in Figure 6(c). The close-view SEM images of n-HApAlgLa beads and fluoride-sorbed n-HApAlgLa beads are presented in Figure 6(d,e), respectively. The composite beads are rough with abundant bumps, and many pores are

Figure 6. Digital pictures of n-HApAlgLa beads in (a) wet and (b) dried nature. (c) SEM picture of the overall shape of n-HApAlgLa bead. Close-view SEM images of (d) n-HApAlgLa beads and (e) fluoride-sorbed n-HApAlgLa beads. EDAX spectra of (f) n-HApAlgLa beads and (g) fluoride-sorbed n-HApAlgLa beads. [Color figure can be viewed in the online issue, which is available at wileyonlinelibrary.com.]
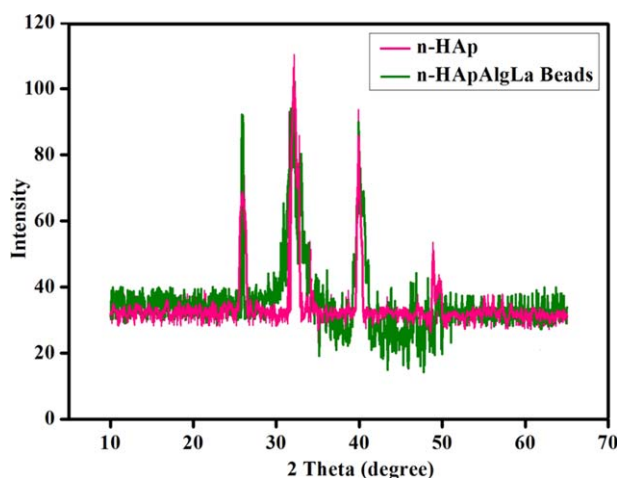
Figure 7. XRD curves of n-HAp and n-HApAlgLa beads. [Color figure can be viewed in the online issue, which is available at wileyonlinelibrary.com.]

present on the surface, which facilitate the diffusion of fluoride ions during sorption. The change in the SEM micrographs of the composite beads and fluoride-treated beads indicates the fluoride sorption. This is further supported by EDAX analysis, which provides the direct confirmation of fluoride sorption onto n-HApAlgLa beads. The EDAX spectra of n-HApAlgLa beads confirm the presence of respective ions in the composite beads (cf. Figure 6f). The fluoride sorption that occurred on n-HApAlgLa beads was confirmed by the presence of fluoride peaks in the EDAX spectra of fluoride-treated n-HApAlgLa beads (cf. Figure 6g). The pH_{zpc} values of n-HAp, n-HApAlg composite, and n-HApAlgLa beads were found to be 7.88, 7.20, and 6.40, respectively. The shift in the pH_{zpc} values confirms the change in surface morphological charges of the material.

XRD curves were used to get the crystallographic information about the sorbent. Figure 7 shows the crystalline peaks of n-HAp at $2\theta = 25.92°$, $32°$, and $39.81°$, which were found in both n-HAp and n-HApAlgLa composites. This signifies that there was no obvious changes in the peak structure after the composite formation and confirmed that the crystal structure of n-HAp was preserved in n-HApAlgLa composite beads.[32]

Sorption Isotherms

The commonly used Freundlich[33] and Langmuir[34] isotherms were applied to describe the fluoride sorption onto n-HApAlgLa beads. The linear forms of isotherms with their plots are given in Table I. The n and k_F values calculated from the slope and intercept of

the linear plot $\log q_e$ vs. $\log C_e$ are presented in Table II. The value of $1/n$ between 0 and 1 and the n values between 1 and 10 represent favorable conditions for sorption. The linear plot of C_e/q_e vs. C_e indicates the applicability of Langmuir isotherm. The values of $Q°$ and b calculated from the slope and the intercept of the plot C_e/q_e vs. C_e are listed in Table II. The increase in the values of $Q°$ and b with the rise in temperature indicates the endothermic nature of fluoride removal. The R_L values lies between 0 and 1 indicate that the sorption process was favorable.[35]

Chi-Square Analysis

To identify the suitable isotherm for sorption of fluoride onto n-HApAlgLa composite, the χ^2 analysis was carried out. The χ^2 test statistic is basically the sum of the squares of the differences between the experimental data and the data obtained by calculating from models, with each squared difference divided by the corresponding data obtained by calculating from the models. The equivalent mathematical statement is as follows:

$$\chi^2 = \sum \frac{(q_e - q_{e,m})^2}{q_{e,m}} \qquad (2)$$

where $q_{e,m}$ is the equilibrium capacity obtained by calculating from the model (mg g^{-1}), and q_e is the experimental data of the equilibrium capacity (mg g^{-1}). If data from the model are similar to the experimental data, χ^2 will be a small number, whereas if they differ, χ^2 will be a bigger number. The results of χ^2 analysis are presented in Table II. The obtained χ^2 values of Langmuir isotherm are lower than Freundlich isotherm, indicating that the fluoride sorption onto n-HApAlgLa beads follows Langmuir isotherm.

Thermodynamic Parameters of Composite Beads

The calculated values of standard free energy change ($\Delta G°$), standard enthalpy change ($\Delta H°$), and standard entropy change ($\Delta S°$) of n-HApAlgLa composite beads were calculated as follows. The free energy of sorption process, considering the sorption equilibrium coefficient K_o, is given by the following equation:

$$\Delta G° = -RT \ln K_o \qquad (3)$$

where $\Delta G°$ is the standard free energy of sorption (kJ mol^{-1}), T is the temperature in Kelvin, and R is the universal gas constant (8.314 J mol^{-1} K^{-1}). The sorption distribution coefficient, K_o, was determined from the slope of the plot $\ln (q_e/C_e)$ against C_e at different temperatures and extrapolating to zero C_e according to the method suggested by Khan and Singh.[36]

Table I. Isotherms and Their Linear Forms

Isotherms		Linear form	Plot	Parameters
Freundlich	$q_e = k_F C_e^{1/n}$	$\log q_e = \log k_F + \frac{1}{n} \log C_e$	$\log q_e$ vs. $\log C_e$	q_e: Amount of fluoride adsorbed per unit weight of the adsorbent (mg g^{-1})
				C_e: Equilibrium concentration of fluoride in solution (mg L^{-1})
				k_F: Measure of adsorption capacity (mg g^{-1})
				$1/n$: Adsorption intensity
Langmuir	$q_e = \frac{Q°bC_e}{1+bC_e}$	$\frac{C_e}{q_e} = \frac{1}{Q°b} + \frac{C_e}{Q°}$	$\frac{C_e}{q_e}$ vs. C_e	$Q°$: Amount of adsorbate at complete monolayer coverage (mg g^{-1})
				b: Langmuir isotherm constant (L mg^{-1})

Table II. Isotherms and Thermodynamic Parameters of n-HApAlgLa Composite Beads

Temperature (°C)	Freundlich isotherm					Langmuir isotherm					Thermodynamic parameters		
	$1/n$	n	k_F (mg g^{-1}) (L mg^{-1})$^{1/n}$	r	χ^2	$Q°$ (mg g^{-1})	b (L g^{-1})	R_L	r	χ^2	$\Delta G°$ (kJ mol^{-1})	$\Delta H°$ (kJ mol^{-1})	$\Delta S°$ (kJ mol^{-1} K^{-1})
30	0.201	4.965	2.889	0.985	0.003	4.536	1.380	0.068	0.999	0.0002	−3.63	6.18	0.01
40	0.202	4.942	3.126	0.990	0.004	4.916	1.417	0.066	0.998	0.001	−3.44		
50	0.237	4.214	3.242	0.957	0.007	5.271	1.442	0.067	0.997	0.003	−3.46		

Table III. Kinetic Models of n-HApAlgLa Composite Beads on Fluoride Removal

Kinetic models	Parameters	30°C				40°C				50°C			
		8 mg L^{-1}	10 mg L^{-1}	12 mg L^{-1}	14 mg L^{-1}	8 mg L^{-1}	10 mg L^{-1}	12 mg L^{-1}	14 mg L^{-1}	8 mg L^{-1}	10 mg L^{-1}	12 mg L^{-1}	14 mg L^{-1}
Pseudo-first-order	k_{ad} (min^{-1})	0.202	0.197	0.160	0.154	0.107	0.059	0.091	0.043	0.086	0.057	0.033	0.035
	r	0.935	0.899	0.897	0.815	0.989	0.983	0.927	0.935	0.987	0.998	0.993	0.967
	SD	0.348	0.436	0.358	0.495	0.073	0.050	0.167	0.074	0.063	0.0156	0.018	0.042
Pseudo-second-order	q_e (mg g^{-1})	3.311	3.802	3.953	4.132	3.401	3.817	4.132	4.255	3.559	3.861	4.184	4.329
	k (g mg^{-1} min^{-1})	0.195	0.153	0.221	0.213	0.199	0.227	0.159	0.199	0.144	0.231	0.180	0.200
	h (mg g^{-1} min^{-1})	2.137	2.208	3.460	3.636	2.299	3.311	2.717	3.597	1.828	3.448	3.145	3.745
	r	1.000	0.999	0.999	0.999	1.000	1.000	0.999	0.999	0.998	1.000	1.000	0.999
	SD	0.075	0.115	0.087	0.112	0.076	0.086	0.126	0.121	0.203	0.066	0.075	0.102
Particle diffusion	k_p (min^{-1})	0.201	0.183	0.153	0.154	0.107	0.059	0.091	0.043	0.084	0.058	0.033	0.035
	r	0.934	0.921	0.903	0.816	0.988	0.982	0.927	0.938	0.989	0.998	0.991	0.971
	SD	0.802	0.811	0.760	1.142	0.172	0.118	0.385	0.166	0.133	0.039	0.045	0.090
Intraparticle diffusion	k_i (mg g^{-1} min$^{-0.5}$)	0.164	0.189	0.130	0.126	0.157	0.129	0.168	0.138	0.177	0.134	0.174	0.137
	r	0.983	0.996	0.987	0.965	0.995	0.996	0.985	0.965	0.977	0.998	0.992	0.979
	SD	0.041	0.024	0.029	0.046	0.022	0.016	0.039	0.050	0.052	0.011	0.030	0.038
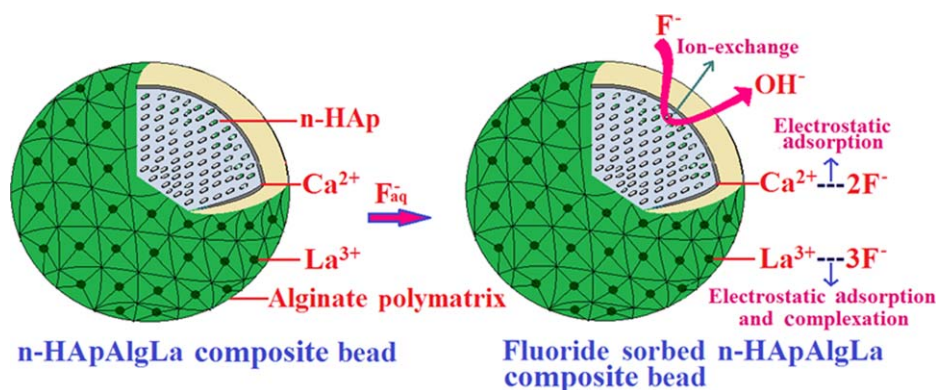
Figure 8. Feasible fluoride removal mechanism of n-HApAlgLa composite beads. [Color figure can be viewed in the online issue, which is available at wileyonlinelibrary.com.]

The sorption distribution coefficient may be expressed in terms of $\Delta H°$ and $\Delta S°$ as a function of temperature:

$$\ln K_o = \frac{\Delta S^o}{R} - \frac{\Delta H^o}{RT} \qquad (4)$$

where $\Delta H°$ is the standard enthalpy change (kJ mol^{-1}) and $\Delta S°$ is the standard entropy change (kJ mol^{-1} K^{-1}). The values of $\Delta H°$ and $\Delta S°$ can be obtained from the slope and intercept of a plot of $\ln K_o$ against $1/T$.

The negative values of $\Delta G°$ and positive values of $\Delta H°$ indicated that the fluoride sorption process is spontaneous and endothermic in nature. The positive value of $\Delta S°$ suggests the increased randomness at the solid–solution interface during the fluoride removal.

Sorption Kinetics

The two main types of sorption kinetic models, namely, reaction-based and diffusion-based models, were adopted to fit the experimental data. The most commonly used pseudo-first-order[37] and pseudo-second-order models were used as reaction-based models.[38] The linear plots of log $(q_e - q_t)$ against t gives straight line, indicating the applicability of pseudo-first-order model. The slope of the straight line plots log $(q_e - q_t)$ against t at different temperatures, namely, 30, 40, and 50°C, give the value of the pseudo-first-order rate constant (k_{ad}), and the r values are listed in Table III. The pseudo-second-order equation can be found out experimentally by plotting t/q_t against t. The values of q_e, k, h, and r of the pseudo-second-order model obtained from the plots of t/q_t vs. t for fluoride sorption at different temperatures, namely, 30, 40, and 50°C, of composite beads are presented in Table III. The values of q_e increase with the increase in temperature, indicating that the fluoride sorption increases with the increase in temperature. The higher r values obtained for pseudo-second-order model than pseudo-first-order model indicate the applicability of the pseudo-second-order model.

For a solid–liquid sorption process, the solute transfer is usually characterized either by particle diffusion[39] or by intraparticle diffusion[40] control. The respective straight line plots of ln $(1 - C_t/C_e)$ vs. t and q_t vs. $t^{0.5}$ indicates the applicability of particle and intraparticle diffusion, respectively. The k_p, k_i, and r values at different temperatures, namely, 30, 40, and 50°C, for

both particle and intraparticle diffusion models are illustrated in Table III. The r values obtained for both particle and intraparticle diffusion models are almost comparable. The normalized SD was often used to evaluate the conformity between experimental data and modeled values. Based on the SD values (cf. Table III), it is clear that the lower SD values of pseudo-
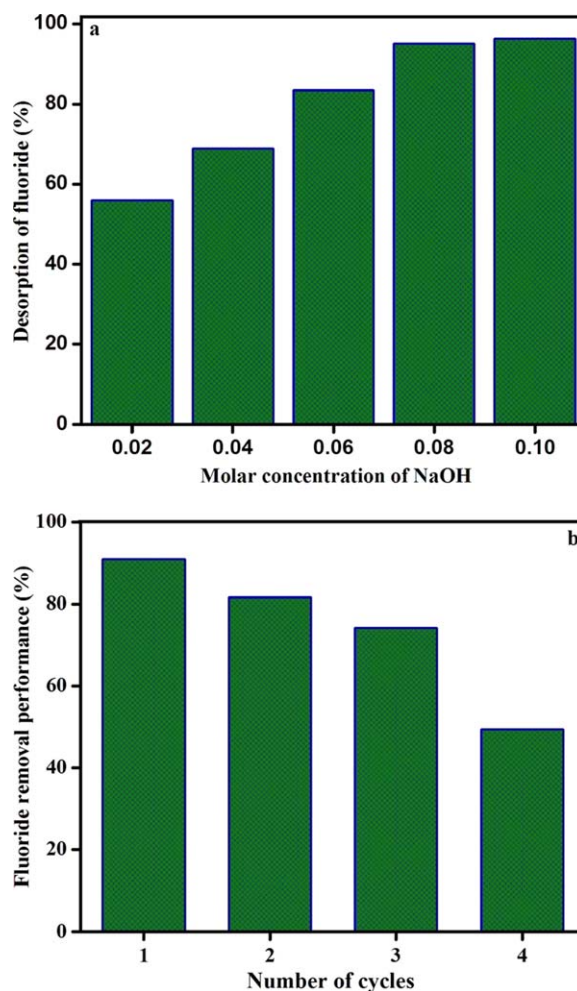
Figure 9. n-HApAlgLa composite (a) regeneration and (b) reusability studies. [Color figure can be viewed in the online issue, which is available at wileyonlinelibrary.com.]

Table IV. Field Studies of n-HApAlgLa Composite Beads

Water quality parameters	Treatment	
	Before	After
F^- (mg L^{-1})	3.07	1.01
pH	8.38	8.07
Cl^- (mg L^{-1})	284	261
SO_4^{2-} (mg L^{-1})	476	459
NO_3^- (mg L^{-1})	68	56
HCO_3^- (mg L^{-1})	219	187
Total hardness (mg L^{-1})	313	252
Total dissolved solids (mg L^{-1})	736	715

second-order and intraparticle diffusion model are suitable for describing the fluoride sorption onto n-HApAlgLa composite beads.

Mechanism of Fluoride Removal by n-HApAlgLa Composite Beads

The feasible mechanism of fluoride removal by n-HApAlgLa composite beads was governed by adsorption, complexation, and ion exchange as shown in Figure 8. The coating of n-HAp with Alg often occurs through hydrogen bonding or metal-complexing mechanism. The positively charged Ca^{2+} ions present in n-HApAlgLa composite beads attracted negatively charged fluoride ions by means of electrostatic attraction, whereas La^{3+} ions remove the fluoride by electrostatic adsorption and complexation. In addition, the OH^- ions present in the n-HAp lattice are replaced by F^- ions through ion-exchange mechanism.

Regeneration and Reusability Studies

Desorption is the recovery of adsorbed materials for reuse. From the pH studies (cf. Figure 3), it is observed that the maximum fluoride sorption occurred at pH ranges 3–5. It is suggested that desorption of fluoride from n-HApAlgLa composite may be attained by dilute alkaline solution as regenerant. The fluoride-treated sorbent has been tested with dilute NaOH for about 40 min with different concentrations ranging from 0.02 to 0.1M. Figure 9a shows that the percentage of desorption increased with the increase in NaOH concentration. Hence, 0.1M NaOH solution can be used as a suitable eluent for the regeneration of the sorbent. The regenerated n-HApAlgLa composite beads has yielded 90.84% of fluoride uptake capacity in first cycle. Thereafter, the fluoride removal percentage has been decreased to 81.56, 74.18, and 49.37% of second, third, and fourth cycles, respectively, as shown in Figure 9b. The decrease in fluoride removal capacity from the first to fourth cycle may be due to the fact that the replaceable OH^- is fully occupied by fluoride ions.

Field Study

To find the suitability of n-HApAlgLa composite beads at field conditions, a water sample collected from a nearby fluoride-prevalent village was tested. About 0.1 g of composite beads was added to 50 mL of fluoride water sample, and the content was shaken with constant time at room temperature. The field trial results are presented in Table IV. n-HApAlgLa composite beads reduce the fluoride concentration below the tolerance limit. Even though the concentration of other anions is higher than fluoride concentration in field water, n-HApAlgLa beads remove fluoride selectively. In addition, there is a significant reduction in the levels of other water quality parameters. Hence, n-HApAlgLa composite beads can be effectively used for removing the fluoride from water.

Comparison with Other Adsorbents

The adsorption capacity of n-HApAlgLa composite beads was compared with other adsorbents reported in the literature, and the results are given in Table V. n-HApAlgLa composite possesses appreciable DC when compared with that of the reported sorbents, which shows its high selectivity toward fluoride.

CONCLUSIONS

In this study, n-HApAlgLa composite was prepared in a usable bead form, which possesses significant potential towards fluoride

Table V. Comparison of the Adsorption Capacity of a Few Reported Adsorbents with n-HApAlgLa Composite Beads

S. No	Adsorbent	Adsorption capacity (mg g^{-1})	Reference
1	Alginate beads filled with nanohydroxyapatite	3.72	This study
2	Manganese oxide-coated alumina	2.85	41
3	Nanohydroxyapatite/chitin composite	2.84	42
4	Activated alumina-doped cellulose acetate phthalate	2.30	43
5	Fe-Al-Ce nanoadsorbent	2.20	44
6	Chitosan-supported zirconium(IV) tungstophosphate composite	2.03	45
7	Nanohydroxyapatite	1.30	50
8	Calcium chloride-modified natural zeolite	1.76	46
9	Protonated chitosan beads	1.66	8
10	Nanohydroxyapatite/chitosan composite	1.56	24
11	Carboxylated chitosan beads	1.39	47
12	Hydrotalcite/chitosan composite	1.26	48
13	Aluminum-impregnated activated carbon	1.07	49

removal. The DC of n-HApAlgLa beads was influenced by pH of the medium and slightly in the presence of bicarbonate ions. The sorption of fluoride onto n-HApAlgLa beads follows Langmuir isotherm. The nature of fluoride removal was spontaneous and endothermic. Kinetic study revealed that fluoride sorption was controlled by pseudo-second-order and intraparticle diffusion models. The mechanism of defluoridation was governed by adsorption, complexation, and ion exchange. The composite beads will overcome the brittleness, poor mechanical strength, and pressure drop during field studies. A study on the regeneration and reuse of n-HApAlgLa composite beads specifies that it is effective up to third cycles without much decline in performance. The synthesized n-HApAlgLa composite beads are low cost, ecofriendly, biodegradable, and biocompatible sorbent for safe drinking water.

REFERENCES

1. W.H.O. Report, Fluoride and Fluorides: Environmental Health Criteria, World Health Organisation, **1984**.

2. Lu, N. C.; Liu, J. C. *Sep. Purif. Technol.* **2010**, *74*, 329.

3. Min, B. R.; Gill, A. L.; Gill, W. N. *Desalination* **1984**, *49*, 89.

4. Vasudevan, S.; Lakshmi, J.; Sozhan, G. *Clean* **2009**, *37*, 372.

5. Simons, R. *Desalination* **1993**, *89*, 325.

6. Meenakshi, S.; Viswanathan, N. *J. Colloid Interface Sci.* **2007**, *308*, 438.

7. Karthikeyan, G.; Siva Ilango, S. *Iran. J. Enviorn. Health. Sci. Eng.* **2007**, *4*, 21.

8. Viswanathan, N.; Sairam Sundaram, C.; Meenakshi, S. *J. Hazard. Mater.* **2009**, *161*, 423.

9. Meski, S.; Ziani, S.; Khireddine, H. *J. Chem. Eng. Data* **2010**, *55*, 3923.

10. Li, S.; Bai, H.; Wang, J.; Jing, X.; Liu, Q.; Zhang, M.; Chen, R.; Liu, L.; Jiao, C. *Chem. Eng. J.* **2012**, *193*, 372.

11. Jayakumar, R.; Rajkumar, M.; Freitas, H.; Selvamurugan, N.; Nair, S. V.; Furuike, T.; Tamura, H. *Int. J. Biol. Macromol.* **2009**, *44*, 107.

12. Viswanathan, N.; Pandi, K.; Meenakshi, S. *Int. J. Biol. Macromol.* **2014**, *70*, 347.

13. Gopalakannan, V.; Viswanathan, N. *Int. J. Biol. Macromol.* **2015**, *72*, 862.

14. Pandi, K.; Viswanathan, N. *Carbohydr. Polym.* **2014**, *112*, 662.

15. Lakouraj, M. M.; Mojerlou, F.; Zare, E. N. *Carbohydr. Polym.* **2014**, *106*, 34.

16. Yang, H.; Li, H.; Zhai, J.; Sun, L.; Zhao, Y.; Yu, H. *Chem. Eng. J.* **2014**, *246*, 10.

17. Li, X.; Qi, Y.; Li, Y.; Zhang, Y.; He, X.; Wang, Y. *Bioresour. Technol.* **2013**, *142*, 611.

18. Jeon, C.; Park, J. Y.; Yoo, Y. J. *Water Res.* **2002**, *36*, 1814.

19. Pandi, K.; Viswanathan, N. *Carbohydr. Polym.* **2015**, *118*, 242.

20. Jiang, N.; Xu, Y.; Dai, Y.; Luo, W.; Dai, L. *J. Hazard. Mater.* **2012**, *215-216*, 17.

21. Min, J. H.; Hering, J. G. *Water Res.* **1998**, *32*, 1544.

22. Zhou, Y.; Yu, C.; Shan, Y. *Sep. Purif. Technol.* **2004**, *36*, 89.

23. Viswanathan, N.; Meenakshi, S. *J. Appl. Polym. Sci.* **2009**, *112*, 1114.

24. Sairam Sundaram, C.; Viswanathan, N.; Meenakshi, S. *Bioresour. Technol.* **2008**, *99*, 8226.

25. American Public Health Association. Standard Methods for the Examination of Water and Waste Water; American Public Health Association: Washington, DC, **2005**.

26. Lopez-Ramon, M. V.; Stoeckli, F.; Moreno-Castilla, C.; Carrasco-Marin, F. *Carbon* **1999**, *37*, 1215.

27. Goh, K.; Lim, T.; Dong, Z. *Water Res.* **2008**, *42*, 1343.

28. Viswanathan, N.; Meenakshi, S. *J. Hazard. Mater.* **2010**, *178*, 226.

29. Ma, M. G.; Zhu, Y. J.; Chang, J. *J. Phys. Chem. B* **2006**, *110*, 14226.

30. Jin, H.; Lee, C.; Lee, W.; Lee, J.; Park, H.; Yoon, S. *Mater. Lett.* **2008**, *62*, 1630.

31. Rajkumar, M.; Meenakshisundaram, N.; Rajendran, V. *Mater. Charact.* **2011**, *62*, 469.

32. Jie, W.; Yubao, L. *Eur. Polym. J.* **2004**, *40*, 509.

33. Freundlich, H. M. F. Z. *Phys. Chem. A* **1906**, *57A*, 385.

34. Langmuir, I. *J. Am. Chem. Soc.* **1916**, *38*, 2221.

35. El Geundi, M. S. *Water Res.* **1991**, *25*, 271.

36. Khan, A. A.; Singh, R. P. *Colloids Surf.* **1987**, *24*, 33.

37. Lagergren, S. K. *Svenska Vetenskapsakad. Handl.* **1898**, *24*, 1.

38. Ho, Y. S.; McKay, G. *Process Biochem.* **1999**, *34*, 451.

39. Chanda, M.; O'Driscoll, K. F.; Rempel, G. M. *React. Polym.* **1983**, *1*, 281.

40. Weber, W. J.; Morris, J. C. *J. Sanitary Eng. Div.* **1964**, *90*, 79.

41. Maliyekkal, S. M.; Sharma, A. K.; Philip, L. *Water Res.* **2006**, *40*, 3497.

42. Sairam Sundaram, C.; Viswanathan, N.; Meenakshi, S. *J. Hazard. Mater.* **2009**, *172*, 147.

43. Chatterjee, S.; De, S. *Sep. Purif. Technol.* **2014**, *125*, 223.

44. Chen, L.; Wu, H.; Wang, T.; Jin, Y.; Zhang, Y.; Dou, X. *Powder Technol.* **2009**, *193*, 59.

45. Viswanathan, N.; Meenakshi, S. *J. Hazard. Mater.* **2010**, *176*, 459.

46. Zhang, Z.; Tan, Y.; Zhong, M. *Desalination* **2011**, *276*, 246.

47. Viswanathan, N.; Sairam Sundaram, C.; Meenakshi, S. *Colloids Surf. B* **2009**, *68*, 48.

48. Viswanathan, N.; Meenakshi, S. *Appl. Clay Sci.* **2010**, *48*, 607.

49. Ramos, R. L.; Ovalle-Turrubiartes, J.; Sanchez-Castillo, M. A. *Carbon* **1999**, *37*, 609.

50. Sairam Sundaram, C.; Viswanathan, N.; Meenakshi, S. *J. Hazard. Mater.* **2008**, *155*, 206.